ACCOUNTS
of chemical research

Anion-Exchangeable Layered Materials Based on Rare-Earth Phosphors: Unique Combination of Rare-Earth Host and Exchangeable Anions

FENGXIA GENG, RENZHI MA, AND TAKAYOSHI SASAKI*

International Center for Materials Nanoarchitectonics, National Institute for Materials Science, 1-1 Namiki, Tsukuba, Ibaraki 305-0044, Japan

RECEIVED ON DECEMBER 17, 2009

CONSPECTUS

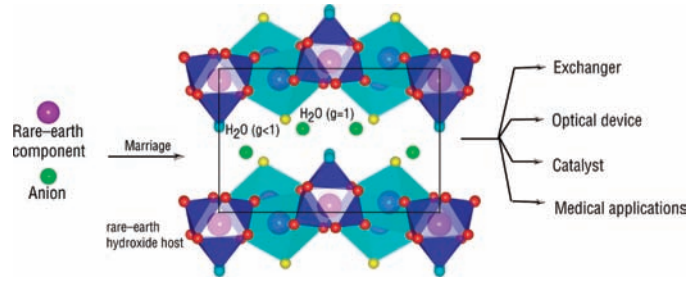

Layered materials, three-dimensional crystals built from stacking two-dimensional components, are attracting intense interest because of their structural anisotropy and the fascinating properties that result. However, the range of such layered materials that can exchange anions is quite small. Continuing efforts have been underway to identify a new class of anion-exchangeable materials. One major goal is the incorporation of rare-earth elements within the host because researchers expect that the marriage of rare-earth skeleton host and the exchangeable species within the interlayer will open up new avenues both for the assembly of layered materials and for the understanding of rare-earth element chemistry. Such lanthanide layered solids have industrial potential. These materials are also of academic importance, serving as an ideal model for studying the cationic size effect on structure stability associated with lanthanide contraction. In this Account, we present the work done by ourselves and others on this novel class of materials. We examine the following four subtopics regarding these layered anionic materials: (1) synthesis strategy and composition diversity, (2) structural features, (3) structure stability with relative humidity, and (4) applications.

These materials can be synthesized either by hydrothermal reactions or by homogeneous precipitation, and a variety of anions can be intercalated into the gallery. Although only cations with a suitable size can form the layered structure, the possible range is wide, from early to late lanthanides. We illustrate the effect of lanthanide contraction on properties including morphology, lattice dimensions, and coordination numbers. Because each lanthanide metal ion coordinates water molecules, and the water molecules point directly into the gallery space, this feature plays a critical role in stabilizing the layered structure. In the 9-fold monocapped square antiprism structure, the humidity-triggered transition between high- and low-hydrated phases corresponds to the uptake of H_2O molecules at the capping site, which provides further evidence of the importance of water coordination.

Applications using this unique combination of rare-earth element chemistry and layered materials include ion-exchange, photoluminescence, catalysis, and biomedical devices. Further exploration of the compounds and new methods for functional modification would dramatically enrich the junction of these two fields, leading to a new generation of layered materials with desirable properties.

Introduction

Anion-exchangeable layered materials are three-dimensional crystals built up from loosely stacked two-dimensional infinite platelets with positive charges that are neutralized by anions accommodated in the gallery. The atoms in the host are held together primarily by covalent bonding so as to form substantially rigid two-dimensional layers, while the electrostatic interaction between the charged layers is much weaker.[1−3] A counterpart to anion-exchangeable layered materials is a cation-exchangeable layered compound comprising

Published on the Web 06/18/2010 www.pubs.acs.org/acr
10.1021/ar900289v

negatively charged layers interspaced with cations. The structural anisotropy endows the materials with rich interlayer chemistry and the unique behavior of swelling and exfoliation into the basic building block: individual layers. Specifically, the ions between the layers can be quantitatively exchanged with others even at ambient conditions with the host structure well conserved, which can lead to measured changes in geometrical, chemical, and electronic environments of either guest or host, and thus enable materials to be tailored to meet specific requirements, such as catalysis, chromatography, drug delivery, and others.[1] The individual layers from exfoliation, referred to as "nanosheets", exhibiting infinite length in the plane and only ~1 nm in thickness, are regarded as a new class of nanoscale materials and are attracting tremendous attention from both experimental and theoretical communities due to their unique properties.[4−6] Graphene, which is one monolayer of carbon atoms, is a particularly fascinating type of nanosheet that may offer a cornucopia of new physics and potential applications.[7]

Because a host layer is typically a two-dimensional crystalline network of polyhedra with a multivalent metal ion center surrounded by anions, the layer surface is always negatively charged, which favors cation insertion between the networks to attain local charge neutrality. Thus, though there is wide occurrence of layered materials showing cation exchange reactivity (such as smectite clays, metal phosphates and phosphonates, metal oxides, and others), examples of anion-exchangeable materials are very limited.[1,8] To make an anion exchanger, the anionic species in the host should have appropriate charge and size to fill the metal coordination sphere while leaving the positive charges of metal centers not completely balanced. Besides the electrostatic forces between the host layer and anions in the gallery, some interactions, for instance, hydrogen bonding, are also required to stabilize the structure. For these reasons, materials with anion exchangeability are available mainly in the form of hydroxides. A typical and widely studied example is layered double hydroxides (LDHs) with the general formula $[M^{2+}_{1-x}M^{3+}_{x}(OH)_2][A^{q-}_{x/q}\cdot mH_2O]$ (M^{2+} and M^{3+} are divalent and trivalent cations, respectively, x is equal to the ratio of $M^{3+}/(M^{2+} + M^{3+})$, A^{q-} is an anion of valence q). The composition is diverse as the general formula suggests, but all components are isostructural and are derived from brucite, $Mg(OH)_2$, which consists of $Mg(OH)_6$ octahedra sharing edges to form infinite charge-neutral layers. Partial substitution of M^{2+} ions in the brucite lattice by M^{3+} renders layers that acquire a positive charge, which is balanced by interlayer counteranions between the two brucite-like slabs, as shown in Figure 1. Water molecules are usually co-intercalated and are hydrogen-bonded to hydroxyls in the host or to the interlayer anions. Although the increasing importance of LDHs in many areas of materials chemistry has been recognized and well documented, the design and discovery of other anion-exchangeable materials remains a formidable challenge. Aluminum-hydroxide-based gibbsite containing mono- and trivalent cations, $LiAl_2(OH)_6A^{q-}_{1/q}$ (A = Cl, Br, NO_3, ...),[9] hydroxy double salts with only divalent metal centers,[10] for example, $ZnCu_{1.5}(OH)_4NO_3$, and some single-metal layered hydroxide salts,[8,11] such as $Co_{1.18}(OH)_2Cl_{0.36}\cdot 0.66H_2O$ (α-$Co(OH)_2$), undergo anion-exchange reactions. In addition, a unique strategy was developed to produce anion exchangers converted from cation ones through excess intercalation of polycations, in which layer charge is overcompensated and the surplus positive charge gives rise to the ability to encapsulate and exchange anionic species.[12,13]

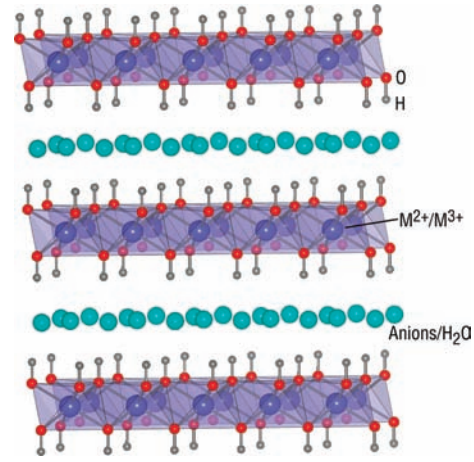

FIGURE 1. Schematic structural representation of LDHs.

The lanthanide elements (Ln), La through Lu, along with their congener Y, are increasingly attractive options for various technological applications ranging from high-performance magnets and luminescent devices to catalysts and other functional materials.[14] Most of these useful functions originate from the unique electron shell structure. The lanthanide series is also of great academic importance because of the linear size reduction both in atoms and in Ln^{3+} ions with an increase in atomic number, known as lanthanide contraction. Such families provide an ideal framework for systematic studies on the effect of metal size on crystal structures and their physical properties. The incorporation of lanthanide elements in the host of a host−guest system is desirable, as success would allow rational design of lanthanide skeleton layers and inorganic/organic pillaring and combine the properties of rare-earth elements and rich interlayer chemistry of layered compounds, thus offering numerous opportunities for design-

ing a framework with the optimal architecture and tunable properties. However, although lanthanide-containing complex ions, for example, $[EuW_{10}O_{36}]^{9-}$, were introduced into the gallery of LDHs by ion-exchange reactions,[15,16] the introduction of lanthanides in the host lattices themselves was rarely successful because of their extremely large size. One example is $Ln(OH)_2A^{q-}{}_{1/q}\cdot mH_2O$ ($m = 0$ or 1), which has been studied in detail since the 1970s.[17−21] The compounds were considered to be analogous and consisting of alternate stacking of $Ln(OH)_2^+$ slabs and anion layers. However, because of their required high coordination number, the lanthanide centers in the host generally have direct anion coordination, for example, a nitrate group acting as a monodentate ligand in $La(OH)_2(NO_3)\cdot H_2O$ or a bidentate ligand in $La(OH)_2(NO_3)$,[21] which prohibits simple anion exchange to other anionic forms.[8] The combination concept was achieved in reality only very recently, with the successful synthesis of exchangeable anions sandwiched by positively charged layers of $[Ln_8(OH)_{20}(H_2O)_n]^{4+}$. Much research has focused on developing this field, including synthetic strategy, structure determination, phase stability, and applications. In this Account, we present up-to-date endeavors pursued by ourselves and others on this intriguing new member of anion-exchangeable layered materials.

Synthesis Strategies and Composition Diversity

Layered compounds of this type with the general composition $Ln_8(OH)_{20}A^{q-}{}_{4/q}\cdot nH_2O$ can basically be prepared in two ways. One, which has been used to obtain various well-crystallized LDH materials,[22,23] involves homogeneous precipitation of lanthanide salts of the desired anionic form with hexamethylenetetramine (HMT, $(CH_2)_6N_4$) under refluxing conditions. OH^- ions are slowly released through the reaction ($(CH_2)_6N_4 + 10H_2O \leftrightarrow 4NH_4^+ + 4OH^- + 6HCHO$). Alternatively, lanthanide salts react with precipitation agents such as NaOH and $(CH_3CH_2)_3N$ under hydrothermal conditions. To promote anion intercalation, the sodium salt of the anion to be incorporated is usually added.

Studies on LDH materials showed that the variety of inorganic and organic anions that can be included in the galleries is quite large, but there is some limit on the absolute radii of metal ions in the host layer, M^{2+} and M^{3+}, as well as on their difference.[3] Similarly, various anions can also be incorporated in the layered rare-earth hydroxides; successful cases include organic disulfonate,[24,25] nitrate,[26−30] chloride,[31−33] and bromide.[33] With regard to cation selection, there is always a metal size limit, and the range differs slightly depending on

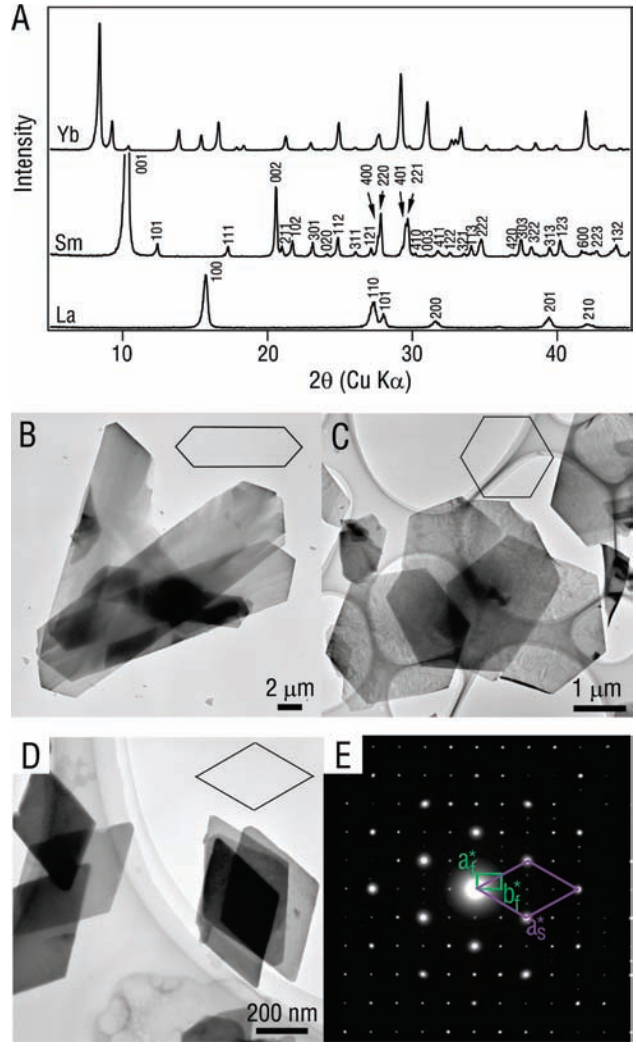

FIGURE 2. (A) Representative XRD patterns of three phases for chloride products from homogeneous precipitation across the series and TEM images of three morphologies for $Ln_8(OH)_{20}(NO_3)_4\cdot nH_2O$ from homogeneous precipitation: (B) large (Sm, Eu, Gd), (C) intermediate (Tb, Dy), and (D) small lanthanides (Ho, Er, Tm). (E) ED pattern taken on one platelet.

the incorporated anions. We systematically studied the products for all 15 elements (La−Lu except Pm, Y) using the homogeneous precipitation method to determine the formation range for the chloride and nitrate series.[28,32] Three different structures, such as $Ln(OH)_3$, the desired layered phase, and other unknown phases, were produced for larger, intermediate, and smaller lanthanides, respectively. This observation is unsurprising considering the gradual variation in physical and chemical behaviors of lanthanide elements as a result of gradual filling of the inner 4f orbital. Figure 2A shows the X-ray diffraction (XRD) patterns of representative samples for the chloride series. Elements ranging from Nd to Tm can form the desired phase, $Ln_8(OH)_{20}Cl_4\cdot nH_2O$. $Nd(OH)_3$ is also present as a minor impurity in the Nd sample (mass percentage 8.1%

from Rietveld analysis). For nitrate cases, elements from Sm to Tm can form the layered phase, $Ln_8(OH)_{20}(NO_3)_4 \cdot nH_2O$. Because pH often plays a critical role in hydrothermal reactions, hydrothermal treatment of $Ln(NO_3) \cdot nH_2O$ and NaOH in the presence of $NaNO_3$ only produces the desired phase for smaller lanthanides, from Gd to Lu and Y,[27] with members extended to Sm and Eu via careful adjustment of pH to around 6.7−7.2.[30] La and Nd members formed from solvothermal reaction of $Ln(NO_3) \cdot nH_2O$ and alkali-metal hydroxide (KOH, RbOH, CsOH) in ethanol media were co-intercalated with alkali-metal nitrates that could be readily removed by subsequent water washing.[34] In the hydrothermal synthesis of samples incorporating bulky organic ions, 2,6-naphthalenedisulfonate and 2,6-anthraquinonedisulfonate, the phases appear to be kinetically favored only by small rare-earth ions (Dy, Ho, Yb, and Y), and the choice of source chemicals for OH^- is decisive. Although amines, such as $(CH_3CH_2)_3N$, can generate the desired layered phase, the product would include a different 3D phase if NaOH is used for precipitation.[24,25]

The morphology also varies with the increase in atomic number as a result of gradual contraction of lanthanide ions, although they all adopt a platelet-like shape.[28,32] As an illustrative example, Figure 2B−D shows the morphological evolution of nitrate samples from homogeneous precipitation. The lateral size tends to decrease with the increase in atomic number, changing from an elongated hexagon (Sm, Eu, Gd) and regular hexagon (Tb, Dy) to a rhombus (Ho, Er, Tm). Characterization of the platelets by TEM and electron diffraction (ED) indicates that each platelet is a single crystal and all samples, regardless of anion identity, yield a similar ED pattern as given in Figure 2E, suggesting their similar in-plane structure. The spots differ in brightness, which is considered to originate from the presence of subcell structures. Specifically, the weaker spots are derived from a rectangular fundamental cell ($a_f \approx$ 13.1 Å; $b_f \approx$ 7.4 Å), and the brighter ones correspond to a subcell with pseudohexagonal symmetry ($a_s \approx$ 3.7 Å).

Structural Features

This section covers the structure determination effort on phases incorporating different anions: chlorides, organic disulfonates, and nitrates. It was generally difficult to produce single crystals large enough for X-ray structure determination, possibly because of their low solubility. Despite extensive variations of synthesis parameters, single crystals of a suitable size were obtained only for $Yb_8(OH)_{20}[C_{14}H_6O_2(SO_3)_2]_2 \cdot 8H_2O$ and $Y_8(OH)_{20}[C_{10}H_6(SO_3)_2]_2 \cdot 8H_2O$.[24] Single-crystal X-ray diffraction study was also performed on extremely small crystals for $Yb_8(OH)_{20}Cl_4 \cdot 6H_2O$ with dimensions of 0.08 × 0.01 × 0.01 mm^3 and 0.05 × 0.04 × 0.005 mm^3 utilizing a special technique with synchrotron-radiated X-ray.[33] For powder samples, a direct method combined with Rietveld fitting was employed for solving the structures in our study.

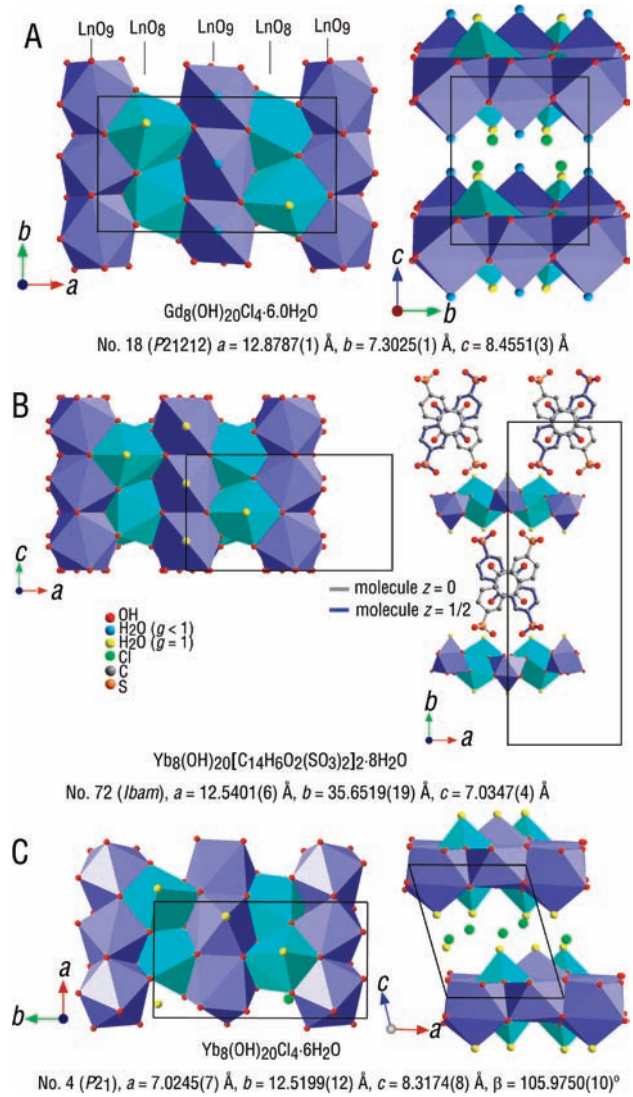

FIGURE 3. Structures for (A) $Gd_8(OH)_{20}Cl_4 \cdot 6.0H_2O$ as an example of chloride series (Nd−Er), (B) $Yb_8(OH)_{20}[C_{14}H_6O_2(SO_3)_2]_2 \cdot 8H_2O$, and (C) monoclinic $Yb_8(OH)_{20}Cl_4 \cdot 6H_2O$. Panels B and C are adapted from refs 24 and 33, respectively. The cell range is set differently for comparison. The 8- and 9-fold polyhedra are in cyan and blue, respectively. The black frames represent unit cells.

Rietveld fitting on our chloride samples from homogeneous precipitation showed that all members (Nd−Er) are isotypic with a primitive orthorhombic symmetry (Figure 3A).[31,32] Consistent with ED observations, the basic metal arrangement is close to the LDH hexagonal symmetry, and deviations from ideal positions lead to a larger orthorhombic cell. Due to the high and flexible coordination number of lanthanides, there are two types of Ln coordination spheres. One is surrounded by seven hydroxyls and one fully occupied H_2O molecule,

forming an 8-fold dodecahedron polyhedron; the second environment has metal centers bonded to eight hydroxyls and one deficient H_2O molecule, forming a 9-fold monocapped square antiprism with the capping position occupied by the H_2O molecule. The reduced occupancy could be induced by repulsion from the neighboring hydroxyls. Polyhedra of the same type are in alternating rows, and each LnO_8 polyhedron is linked to two other LnO_8 and four LnO_9 polyhedra via edge sharing, resulting in corrugated charged slabs.

Phases incorporating organic disulfonates, $Yb_8(OH)_{20}[C_{14}H_6O_2(SO_3)_2]_2 \cdot 8H_2O$ and $Y_8(OH)_{20}[C_{10}H_6(SO_3)_2]_2 \cdot 8H_2O$, also crystallize in orthorhombic symmetry, and each host layer structure is analogous to that of chloride phases; however, double-layer repetition is adopted, involving the gliding of host layers (Figure 3B).[24] For nitrate phases, the structure has not yet been completely solved, but indexing of the XRD patterns suggest monoclinic symmetry, possibly with a slight shift between adjacent layers.[27,28]

As the size of lanthanide centers gradually decrease from early to late lanthanides, structural evolution trend and phase stability with respect to metal size would be of great importance to fundamental research. Several aspects of the chloride series were studied: lattice dimensions, coordination numbers, etc.[32] In-plane lattice parameters exhibited the expected linear decrease with the decrease in rare-earth cation size, whereas two distinct interlamellar distances, ~8.70 and 8.45 Å, were observed for early lanthanides from Nd to Gd and late lanthanides from Tb to Er, respectively, which is considered to be associated with different degrees of hydration, referred to as high-hydrated (HH) and low-hydrated (LH) phases. We elucidated the origin of the interlamellar difference through occupancy refinement of H_2O sites. The variation in water content was found to be correlated with the capping H_2O in the 9-fold monocapped square antiprism. While the ideal total hydration number per chemical formula is 8 with all the H_2O sites fully occupied, 4 from 8-fold and 4 from 9-fold coordination, the refined hydration number for HH and LH Gd samples is 6.6 and 6.0, respectively.[35] The hydration decrease is accompanied by a basal contraction of ~0.2 Å.

Across the series, because the above-mentioned repulsion imposed on the capping H_2O site by neighboring hydroxyls in the 9-fold monocapped square antiprism typically increases with the decrease in size of lanthanide centers, the hydration number gradually decreased with 7.4, 6.3, and 7.2 for HH Nd, Sm, and Eu samples, and 5.8, 5.6, 5.4, and 4.9 for LH Tb, Dy, Ho, and Er samples, respectively. Particularly, the occupancy of the capping H_2O site was only ~0.2 for the right-end pure sample, Er, suggesting that the Er coordination sphere is crowded enough and it might be the lower limit of structure stability based on the size of lanthanide ions. A recent structural study on single crystals of Yb samples from hydrothermal synthesis reported the coexistence of orthorhombic and monoclinic phases with the same composition.[33] The orthorhombic phase possessed a structure ($Pca2_1$) nearly the same as that of earlier members,[36] whereas the metal coordination environment of the monoclinic phase showing a shift between adjacent slabs differed slightly. Among the lanthanide centers that are bonded to eight OH^- and one H_2O site, half lose their water coordination and become saturated with only eight hydroxyls (Figure 3C). This observation, along with the occurrence of transition from HH to LH phase upon decreasing occupancy of bound H_2O sites to a limit described above, demonstrates the critical supporting role played by H_2O molecules. It is speculated that the complete loss of bound H_2O molecules may result in total collapse of the layered structure and that a different phase, probably with a lower coordination number, is preferable for even heavier (smaller) lanthanides, as suggested by the XRD patterns of Yb and Lu samples from homogeneous precipitation. It is interesting to note that, across the series, the metal coordination number of the yielded compounds steadily decreases from 9 only ($Ln(OH)_3$ for La−Pr), to 9 and 8 ($Ln_8(OH)_{20}Cl_4 \cdot xH_2O$ for Nd−Tm) and 8 or less (another phase for Yb and Lu), which reflects the effect of lanthanide contraction.

A close inspection of the varieties of structures immediately reveals that all members of this rare-earth layered family can be viewed as positively charged layers of $[Ln_8(OH)_{20}(H_2O)_n]^{4+}$ and charge-balancing ions sandwiched between the layers, similar to LDHs composed of alternate layers of $[M^{2+}_{1-x}M^{3+}_x(OH)_2]^{x+}$ and anions residing in the gallery, providing possibilities for simple interlayer chemistry (vide post). Still, a structural comparison with LDHs reveals three unexpected and interesting features: (1) Each metal is bound with one water molecule, and the H_2O molecule is pointing toward the gallery space; thus, water might be a key to the stabilization of the layered structure. (2) Distinct from the substantially disordered gallery of LDHs, including both anions and H_2O molecules, the interlayer region in the rare-earth hydroxides is well-ordered, showing electron density corresponding to H_2O and Cl^- in a localized and nearly spherical distribution. (3) In great contrast to LDHs, in which the hexagonal cell is generally preserved for various anions, the structures of the $Ln_8(OH)_{20}A^{q-}_{4/q} \cdot nH_2O$ family vary, depending on the identity of both lanthanide cations and intercalated anions.

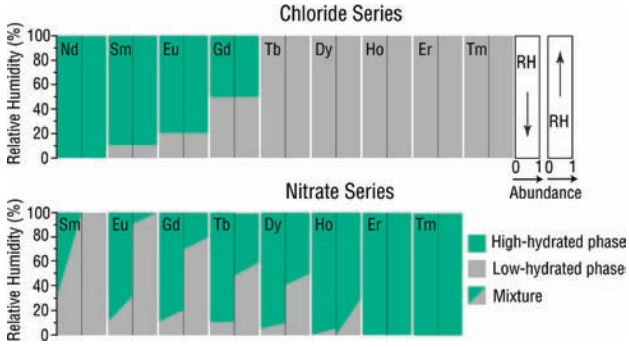

FIGURE 4. Phase changes with RH for Cl^- and NO_3^- series.

Structure Stability with Relative Humidity (RH)

While H_2O molecules usually move freely within the gallery in other layered materials,[3] they are fixed in positions in the family of rare-earth hydroxides and are directly coordinated to the lanthanide centers in the host, thus serving an important role in stabilizing the layered structure, as stated in the former crystallographic refinement section. In this context, the humidity-dependent behavior was monitored by means of XRD and gravimetry characterization. Concomitant abrupt shift in basal spacing and change in sample weight were observed at critical RH, which likely originated from the transition between HH and LH phases. Figure 4 shows the phases adopted in a cycle of decreasing RH from 95% to 5% followed by increasing to 95%. For the chloride series, a larger lanthanide, the Nd sample, tends to adopt HH phase; intermediate lanthanides, Sm, Eu, and Gd samples, exhibit readily reversible conversion between HH and LH phases at critical RH of 10%, 20%, and 50%; and smaller lanthanides favor LH phases.[32] The trend corroborates the repulsion increase exerted on the capping H_2O molecule by neighboring hydroxyls in the 9-fold monocapped square antiprism from early to late lanthanides. The phase conversion finishes within several minutes, roughly 15 min for the Sm sample and less than 2 min for the Eu and Gd samples.

In addition to the repulsion contributing to H_2O loss at low RH, the interlayer anions hydrogen-bonded to the 9-fold antiprism may also be responsible. We substantiate this point with the study on the nitrate series. While an abrupt shift in basal spacing and change in sample weight triggered by RH can be observed, the behavior differs from that of chloride members in three aspects.[28] First, the spacing difference between HH and LH phases is larger, ~0.6 Å. Second, the transition generally starts at a critical RH, but only partial transition occurs with the coexistence of two sets of basal spacing. It does not proceed even after being stored overnight, unless there is a further change in the RH level. Third, distinct from the promptly reversible phase transition in the chloride system, RH hysteresis exists. The differences provide strong indications that additional factors are involved in the phase transition process, presumably a switch in anion configuration. NO_3^-, a flat anion, may tend to adopt a perpendicular position or tilted orientation in HH phases with larger spacing, while a lying-flat configuration is preferred in LH phases. Surprisingly, the nitrate series exhibits an opposite trend to that in the chloride system; that is, critical RH for phase conversion decreases and the RH hysteresis loop becomes smaller with increasing atomic number, suggesting an increase in stability of HH phases. The strength and geometry of hydrogen bonding were found to remarkably affect the hydration ability of a tricapped trigonal prism,[37] which may also be the case for the current monocapped square antiprism. Due to the different geometry of anions, the hydrogen-bonding network formed between NO_3^- and the host certainly differs from that for spherical Cl^-, which may help to stabilize the 9-fold antiprism and thus give rise to the stable HH phases of late lanthanides. Meanwhile, with decreasing atomic number and continuous enlargement of in-plane dimensions, the positive layer charge density (ξ) gradually decreases, generating more available space in the gallery and relatively looser packing of counterbalancing anions. As a result, the earlier lanthanides show a higher tendency for NO_3^- to lie flat, allowing a subtle increase in critical RH for transitions between HH and LH phases.

Applications

The unique combination of two previously unconnected research fields, rare-earth chemistry and interlayer chemistry, may enable the advantages of these two systems to be integrated, thus offering remarkable potential for a wide range of applications in new fields. This section focuses on the possible applications.

A. Interlayer Chemistry. Anion exchange, which is unusual for inorganic materials, has wide industrial application. As detailed earlier, this new family of compounds has a structural feature in common with a typical example of anion-exchangeable compounds, LDHs, namely, free anions included in the gallery. Although ξ of rare-earth hydroxides (~4.1−4.4 × 10^{-2} e/Å^2) is larger than that for LDHs (~4.1 × 10^{-2} e/Å^2 for highest ξ in LDHs series Mg_2Al-LDH, ~3.2 × 10^{-2} e/Å^2 for Mg_3Al-LDH),[38] this does not prevent the layered family from exchangeability comparable to that of LDHs, with interlayer Cl^- and NO_3^- readily exchangeable with other inorganic and organic anions at room temperature (Figure 5A).[27,31] The exchange can be simply achieved by immers-

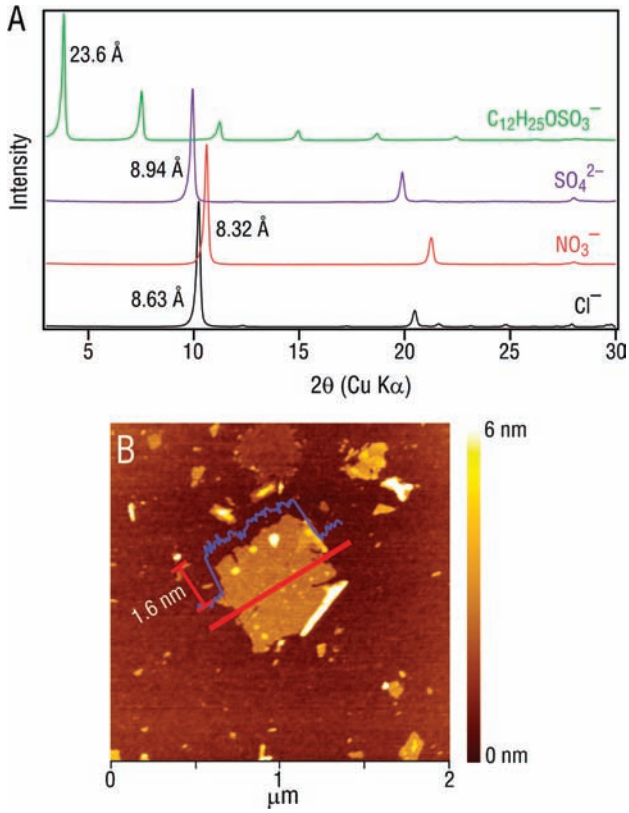

FIGURE 5. (A) XRD patterns of as-obtained Cl^- intercalated and anion-exchanged samples. (B) Atomic force microscopy (AFM) image of nanosheets from exfoliation in formamide after exchanging the anion into $C_{12}H_{25}OSO_3^-$. Adapted from ref 39.

ing the samples in aqueous solution containing the sodium salt of the desired anions in excessive dosage. One notable advantage of rare-earth hydroxides is that no special attention needs to be paid to contamination from carbon dioxide or carbonate, which is a major nuisance in LDH chemistry.[1] This can probably be attributed to their different solubility in water. Rare-earth hydroxides are almost insoluble, whereas LDHs are sparingly soluble and the release of OH anions from base dissociation reactions facilitates the incorporation of carbonate. This layered family can be considered as an additional member of anion-exchangeable compounds, useful for ion-exchange or storage materials.

It is known that layered materials tend to swell and exfoliate into nanosheets in water or organic solvent under certain conditions. Similar to the procedures applicable for LDHs, the rare-earth hydroxides can be delaminated into single unilamellar nanosheets 1.6 nm in thickness in formamide after exchanging the interlayer anions with dodecylsulfonate,[39] as shown in Figure 5B. Stable colloidal aqueous suspension of $Gd_8(OH)_{20}(H_2O)_{7.0}$ nanosheets of bi- or trilayers can be obtained by ultrasonication treatment of the precipitate slurry obtained from postreaction centrifugation.[40] The

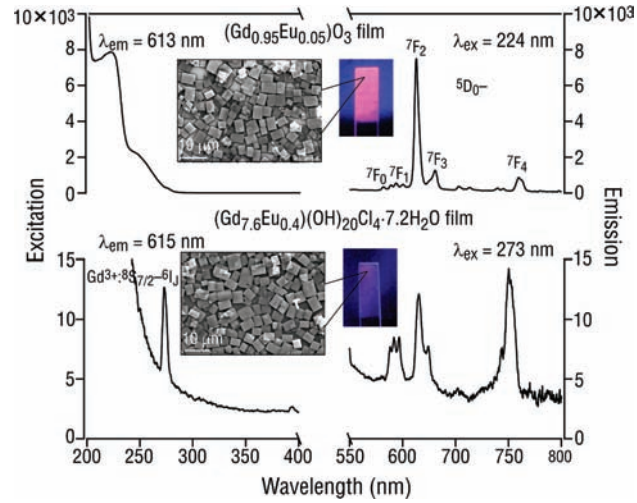

FIGURE 6. Excitation and emission spectra for films of $(Gd_{7.6}Eu_{0.4})(OH)_{20}Cl_4 \cdot 7.2H_2O$ (bottom) and $(Gd_{0.95}Eu_{0.05})_2O_3$ (top). Insets are the corresponding SEM images and emission photographs under UV irradiation. Adapted from ref 43.

nanosheets can also be generated by dispersing in a nonpolar organic solvent after exchanging mother NO_3^- with oleate ions.[41]

B. Photoluminescence Behavior. Eu^{3+} and Tb^{3+} exhibit red and green line-like emissions, respectively, which is of great interest for optical devices. Much effort has been invested in the development of new materials exhibiting emissions in the visible region. The layered rare-earth hydroxides, with rare-earth centers in the host, represent a new class of luminescent materials. The nascent Eu- and Tb-based samples, regardless of anions, show typical Eu^{3+} red and Tb^{3+} green emissions. One problem is that water molecules and hydroxyls are directly coordinated to the lanthanide metal centers, which imposes a drastic quenching effect on the emissions, and thus the emissions are far from industrial requirements. One strategy to address this disadvantage involves post-treatment. In our initial study, an oriented film of layered rare-earth hydroxide platelets was prepared via self-assembly at a hexane/water interface, with photoluminescence and anion-exchange properties preserved.[42] Recently, we demonstrated that densely packed $(Gd_{0.95}Eu_{0.05})_2O_3$ film from annealing treatment of $(Gd_{7.6}Eu_{0.4})(OH)_{20}Cl_4 \cdot 7.2H_2O$ exhibits emission intensity 527 times that of precursor powder samples (Figure 6).[43] Interestingly, the conversion is quasi-topotactic with a close metal arrangement between the (001) lattice plane of the precursor hydroxide and (111) plane of annealed oxide crystals.

C. Catalysis. Catalytic activity of lanthanide compounds is also a fascinating area. $Yb_8(OH)_{20}[C_{14}H_6O_2(SO_3)_2]_2 \cdot 8H_2O$ and $Y_8(OH)_{20}[C_{10}H_6(SO_3)_2]_2 \cdot 8H_2O$ were reported to combine the

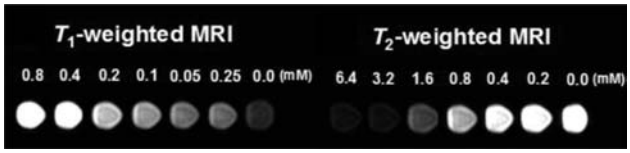

FIGURE 7. T_1- and T_2-weighted MRIs obtained from aqueous suspensions of $Gd_8(OH)_{20}(H_2O)_{7.0}$ nanosheets. Reproduced with permission from ref 40. Copyright 2009 Royal Society of Chemistry.

catalytic properties of rare-earth atoms with the advantages of a solid catalyst, serving as excellent heterogeneous catalysts in green chemistry.[24,25] Three key processes were tested: (1) Hydrodesulfurization of thiophene. $Yb_8(OH)_{20}[C_{14}H_6O_2(SO_3)_2]_2 \cdot 8H_2O$ achieved 50% conversion to hydrogen sulfide and butane in 26 h under much milder conditions (7 bar of H_2 at only 70 °C). (2) Oxidation of sulfides. In the alternative desulfurization reaction, the catalyst showed better activity and selectivity than the previous rare-earth succinate polymeric framework, with a small quantity of required catalyst and fast substrate conversion. (3) Oxidation of linalool. $Y_8(OH)_{20}[C_{10}H_6(SO_3)_2]_2 \cdot 8H_2O$ acts as a bifunctional redox-acid catalyst, demonstrating more than 80% conversion to pyranoid and furanoid over 24 h.

D. Medical Applications. The use of lanthanide complexes as a magnetic resonance imaging (MRI) contrast agent has proven to be invaluable in the diagnosis of several internal abnormalities.[44] Among the lanthanide series, Gd^{3+} stands out because of its unique nature: high effective magnetic moment (seven unpaired electrons) and slow electronic relaxation rate from its symmetric S-state.[44,45] The potential application of the layered rare-earth hydroxides as a new MRI contrast agent was studied using an aqueous nanosheet suspension of $Gd_8(OH)_{20}Cl_4 \cdot 7.0H_2O$.[40] The suspension proved to be a potential T_1-weighted agent with low r_2/r_1 ratio, 3.1, along with sufficient r_1 value (r_1 and r_2, amount of increase in $1/T_1$ and $1/T_2$, respectively, per unit concentration of agent) (Figure 7). The high relaxivity is likely due to the high portion of water ligands, one site to each metal, exposed on the surface of the nanosheets.

Concluding Remarks and Outlook

The combination of rare-earth phosphors and exchangeable ions is a unique feature of this layered rare-earth hydroxides family, and it has attracted considerable interest not only in the academic field but also in various practical areas. In this Account, we have highlighted recent efforts by our group and others toward understanding its structural features and properties. The members of the anion-exchangeable family are enriched. All the structures, although with slight variations, consist of a positively charged slab of $[Ln_8(OH)_{20}(H_2O)_n]^{4+}$ and well-ordered charge-balancing ions in the gallery. The direct water coordination in the host distinguishes the compounds from other anion-exchangeable materials, and humidity-dependent behavior is elucidated, which we believe represents a major step forward in bridging two important fields, interlayer chemistry and rare-earth chemistry. By studying the structural evolution trends across the lanthanide series with the gradual change in metal ion radii, we have been able to demonstrate the gradual decrease in in-plane dimensions, coordination numbers, etc., and phase stability with cationic size and water coordination. With the effective coupling of rare-earth hydroxide host and anion exchangeability, various applications such as ion-exchange, photoluminescence, catalysis, and magnetism are exciting prospects. Despite all the progress achieved, it is only the start. Many fundamental issues remain to be addressed to fully utilize the advantages of the combination, such as the host−guest interaction that may be responsible for the structural variations and may impose effects on the HH−LH phase transition. In the future, we believe, layered rare-earth hydroxides will reveal more interesting aspects in both layered solids and rare-earth chemistry and proliferate even wide-ranging applications.

BIOGRAPHICAL INFORMATION

Fengxia Geng received her Masters degree from the Institute of Metal Research, Chinese Academy of Sciences, in 2006. She then joined Professor Takayoshi Sasaki's research group at the National Institute for Materials Science (NIMS) as a Ph.D. candidate and completed her degree from the University of Tsukuba in 2009. Her research is focused on the development and study of new anion-exchangeable layered materials based on rare-earth phosphors.

Renzhi Ma received his Ph.D. degree in materials processing engineering from Tsinghua University (Beijing) in 2000. He worked as a postdoctoral researcher for three years at NIMS, Japan. He is currently a MANA scientist at the International Center for Materials Nanoarchitectonics (MANA), NIMS. His work focuses on the synthetic chemistry and microscopy of inorganic nanotubes and nanosheets.

Takayoshi Sasaki received his Ph.D. degree in chemistry from the University of Tokyo in 1985. Since 1980, he has worked for the National Institute for Research in Inorganic Materials (NIRIM), Japan, which is now NIMS. In 2009, he was appointed as a NIMS fellow. His recent interest has focused on nanosheets obtained by delaminating layered materials.

FOOTNOTES

*To whom correspondence should be addressed. Fax: (+81) 29-854-9061. E-mail: SASAKI.Takayoshi@nims.go.jp.

REFERENCES

1 O'Hare, D. In *Inorganic Materials*; Bruce, D. W., O'Hare, D., Eds.; John Wiley & Sons Ltd.: West Sussex, England, 1997; pp 172−254.

2 Evans, D. G.; Slade, R. C. T. In *Layered Double Hydroxides*; Duan, X., Evans, D. G., Eds.; Springer-Verlag: New York, 2006; pp 1−87.

3 Braterman, P. S.; Xu, Z. P.; Yarberry, F. In *Handbook of Layered Materials*; Auerbach, S. M., Carrado, K. A., Dutta, P. K., Eds.; Marcel Dekker, Inc.: New York, Basel, 2004; pp 373−474.

4 Sasaki, T. Fabrication of Nanostructured Functional Materials Using Exfoliated Nanosheets as a Building Block. *J. Ceram. Soc. Jpn.* **2007**, *115*, 9–16.

5 Ma, R.; Liu, Z.; Li, L.; Iyi, N.; Sasaki, T. Exfoliating Layered Double Hydroxides in Formamide: A Method to Obtain Positively Charged Nanosheets. *J. Mater. Chem.* **2006**, *16*, 3809–3813.

6 Osada, M.; Sasaki, T. Exfoliated Oxide Nanosheets: New Solution to Nanoelectronics. *J. Mater. Chem.* **2009**, *19*, 2503–2511.

7 Geim, A. K.; Novoselov, K. S. The Rise of Graphene. *Nat. Mater.* **2007**, *6*, 183–191.

8 Newman, S. P.; Jones, W. Comparative Study of Some Layered Hydroxide Salts Containing Exchangeable Interlayer Anions. *J. Solid State Chem.* **1999**, *148*, 26–40.

9 Besserguenev, A. V.; Fogg, A. M.; Francis, R. J.; Price, S. J.; O'Hare, D.; Isupov, V. P.; Tolochko, B. P. Synthesis and Structure of the Gibbsite Intercalation Compounds $[LiAl_2(OH)_6]X$ {X = Cl, Br, NO_3} and $[LiAl_2(OH)_6]Cl \cdot H_2O$ Using Synchrotron X-ray and Neutron Powder Diffraction. *Chem. Mater.* **1997**, *9*, 241–247.

10 Meyn, M.; Beneke, K.; Lagaly, G. Anion-Exchange Reactions of Hydroxy Double Salts. *Inorg. Chem.* **1993**, *32*, 1209–1215.

11 Ma, R.; Liu, Z.; Takada, K.; Fukuda, K.; Ebina, Y.; Bando, Y.; Sasaki, T. Tetrahedral Co(II) Coordination in α-Type Cobalt Hydroxide: Rietveld Refinement and X-ray Absorption Spectroscopy. *Inorg. Chem.* **2006**, *45*, 3964.

12 Darder, M.; Colilla, M.; Ruiz-Hitzky, E. Biopolymer-Clay Nanocomposites Based on Chitosan Intercalated in Montmorillonite. *Chem. Mater.* **2003**, *15*, 3774–3780.

13 Hata, H.; Kobayashi, Y.; Mallouk, T. E. Encapsulation of Anionic Dye Molecules by a Swelling Fluoromica through Intercalation of Cationic Polyelectrolytes. *Chem. Mater.* **2007**, *19*, 79–87.

14 Bünzli, J.-C. G. Benefiting from the Unique Properties of Lanthanide Ions. *Acc. Chem. Res.* **2006**, *39*, 53–61.

15 Gago, S.; Pillinger, M.; Ferreira, R. A. S.; Carlos, L. D.; Santos, T. M.; Goncalves, I. S. Immobilization of Lanthanide Ions in a Pillared Layered Double Hydroxide. *Chem. Mater.* **2005**, *17*, 5803–5809.

16 Sousa, F. L.; Pillinger, M.; Ferreira, R. A. S.; Granadeiro, C. M.; Cavaleiro, A. M. V.; Rocha, J.; Carlos, L. D.; Trindade, T.; Nogueira, H. I. S. Luminescent Polyoxotungstoeuropate Anion-Pillared Layered Double Hydroxides. *Eur. J. Inorg. Chem.* **2006**, 726–734.

17 Klevtsova, R. F.; Klevtsov, P. V. X-Ray Diffraction Study of a New Modification of Yttrium Hydroxychloride $Y(OH)_2Cl$. *J. Struct. Chem.* **1967**, *7*, 524–527.

18 Haschke, J. M. Preparation, Phase Equilibria, Crystal Chemistry, and Some Properties of Lanthanide Hydroxide Nitrates. *Inorg. Chem.* **1974**, *13*, 1812–1818.

19 Lundberg, M.; Skarnulis, A. J. The Crystal Structure of $Pr(OH)_2NO_3$. *Acta Crystallogr.* **1976**, *B32*, 2944–2947.

20 Mullica, D. F.; Sappenfield, E. L.; Grossie, D. A. Crystal Structure of Neodymium and Gadolinium Dihydroxy-nitrate, $Ln(OH)_2NO_3$. *J. Solid State Chem.* **1986**, *63*, 231–236.

21 Louër, M.; Louër, D.; Delgado, A. L.; Martinez, O. G. The Structures of Lanthanum Hydroxide Nitrates Investigated by the Rietveld Profile Refinement Technique. *Eur. J. Solid State Inorg. Chem.* **1989**, *26*, 241–253.

22 Iyi, N.; Matsumoto, T.; Kaneko, Y.; Kitamura, K. A Novel Synthetic Route to Layered Double Hydroxides Using Hexamethylenetetramine. *Chem. Lett.* **2004**, *33*, 1122–1123.

23 Ma, R.; Liu, Z.; Takada, K.; Iyi, N.; Bando, Y.; Sasaki, T. Synthesis and Exfoliation of Co^{2+}−Fe^{3+} Layered Double Hydroxides: An Innovative Topochemical Approach. *J. Am. Chem. Soc.* **2007**, *129*, 5257–5263.

24 Gándara, F.; Perles, J.; Snejko, N.; Iglesias, M.; Gómez-Lor, B.; Gutiérrez-Puebla, E.; Monge, M. Á. Layered Rare-Earth Hydroxides: A Class of Pillared Crystalline Compounds for Intercalation Chemistry. *Angew. Chem., Int. Ed.* **2006**, *45*, 7998–8001.

25 Gándara, F.; Puebla, E. G.; Iglesias, M.; Proserpio, D. M.; Snejko, N.; Monge, M. Á. Controlling the Structure of Arenedisulfonates toward Catalytically Active Materials. *Chem. Mater.* **2009**, *21*, 655–661.

26 McIntyre, L. J.; Jackson, L. K.; Fogg, A. M. Synthesis and Anion Exchange Chemistry of New Intercalation Hosts Containing Lanthanide Cations, $Ln_2(OH)_5(NO_3) \cdot xH_2O$ (Ln = Y, Gd-Lu). *J. Phys. Chem. Solids* **2008**, *69*, 1070–1074.

27 McIntyre, L. J.; Jackson, L. K.; Fogg, A. M. $Ln_2(OH)_5NO_3 \cdot xH_2O$ (Ln = Y, Gd-Lu): A Novel Family of Anion Exchange Intercalation Hosts. *Chem. Mater.* **2008**, *20*, 335–340.

28 Geng, F.; Matsushita, Y.; Ma, R.; Xin, H.; Tanaka, M.; Iyi, N.; Sasaki, T. Synthesis and Properties of Well-Crystallized Layered Rare-Earth Hydroxide Nitrates from Homogeneous Precipitation. *Inorg. Chem.* **2009**, *48*, 6724–6730.

29 Hindocha, S. A.; McIntyre, L. J.; Fogg, A. M. Precipitation Synthesis of Lanthanide Hydroxynitrate Anion Exchange Materials, $Ln_2(OH)_5NO_3 \cdot H_2O$ (Ln = Y, Eu-Er). *J. Solid State Chem.* **2009**, *182*, 1070–1074.

30 Lee, K.-H.; Byeon, S.-H. Extended Members of the Layered Rare-Earth Hydroxide Family, $RE_2(OH)_5NO_3 \cdot nH_2O$ (RE = Sm, Eu, and Gd): Synthesis and Anion-Exchange Behavior. *Eur. J. Inorg. Chem.* **2009**, 929–936.

31 Geng, F.; Xin, H.; Matsushita, Y.; Ma, R.; Tanaka, M.; Izumi, F.; Iyi, N.; Sasaki, T. New Layered Rare-Earth Hydroxides with Anion-Exchange Properties. *Chem.—Eur. J.* **2008**, *14*, 9255–9260.

32 Geng, F.; Matsushita, Y.; Ma, R.; Xin, H.; Tanaka, M.; Izumi, F.; Iyi, N.; Sasaki, T. General Synthesis and Structural Evolution of a Layered Family of $Ln_8(OH)_{20}Cl_4 \cdot nH_2O$ (Ln = Nd, Sm, Eu, Gd, Tb, Dy, Ho, Er, Tm, and Y). *J. Am. Chem. Soc.* **2008**, *130*, 16344–16350.

33 Poudret, L.; Prior, T. J.; McIntyre, L. J.; Fogg, A. M. Synthesis and Crystal Structures of New Lanthanide Hydroxyhalide Anion Exchange Materials, $Ln_2(OH)_5X \cdot 1.5H_2O$ (X = Cl, Br; Ln = Y, Dy, Er, Yb). *Chem. Mater.* **2008**, *20*, 7447–7453.

34 Lee, K.-H.; Byeon, S.-H. Synthesis and Aqueous Colloidal Solutions of $RE_2(OH)_5NO_3 \cdot nH_2O$ (RE = Nd and La). *Eur. J. Inorg. Chem.* **2009**, 4727–4732.

35 The Gd sample was chosen because it marks the boundary between members of HH and LH phases.

36 There is a subtle difference between the two structures: because the two rows of 8-fold lanthanide centers are related with a two-fold rotation axis along *z* or two-fold screw axis along *x* in $P2_12_12$, while with glide plane *c* in $Pca2_1$, the chirality of coordination environment is just opposite.

37 Abbasi, A.; Lindqvist-Reis, P.; Eriksson, L.; Sandström, D.; Lidin, S.; Persson, I.; Sandström, M. Highly Hydrated Cations: Deficiency, Mobility, and Coordination of Water in Crystalline Nonahydrated Scandium(III), Yttrium(III), and Lanthanoid(III) Trifluoromethanesulfonates. *Chem.—Eur. J.* **2005**, *11*, 4065–4077.

38 Xu, Z. P.; Zeng, H. C. Abrupt Structural Transformation in Hydrotalcite-like Compounds $Mg_{1-x}Al_x(OH)_2(NO_3)_x \cdot nH_2O$ as a Continuous Function of Nitrate Anions. *J. Phys. Chem. B* **2001**, *105*, 1743–1749.

39 Hu, L.; Ma, R.; Ozawa, T. C.; Sasaki, T. Exfoliation of Layered Europium Hydroxide into Unilamellar Nanosheets. *Chem.—Asian J.* **2010**, *5*, 248–251.

40 Lee, B.-I.; Lee, K. S.; Lee, J. H.; Lee, I. S.; Byeon, S.-H. Synthesis of Colloidal Aqueous Suspensions of a Layered Gadolinium Hydroxide: a Potential MRI Contrast Agent. *Dalton Trans.* **2009**, 2490–2495; http://dx.doi.org/10.1039/b823172a.

41 Yoon, Y.-S.; Lee, B.-I.; Lee, K. S.; Im, G. H.; Byeon, S.-H.; Lee, J. H.; Lee, I. S. Surface Modification of Exfoliated Layered Gadolinium Hydroxide for the Development of Multimodal Contrast Agents for MRI and Fluorescence Imaging. *Adv. Funct. Mater.* **2009**, *19*, 3375–3380.

42 Hu, L.; Ma, R.; Ozawa, T. C.; Geng, F.; Iyi, N.; Sasaki, T. Oriented Films of Layered Rare-Earth Hydroxide Crystallites Self-Assembled at the Hexane/Water Interface. *Chem. Commun.* **2008**, 4897–4899.

43 Hu, L.; Ma, R.; Ozawa, T. C.; Sasaki, T. Oriented Monolayer Film of Gd_2O_3:0.05Eu Crystallites: Quasi-Topotactic Transformation of the Hydroxide Film and Drastic Enhancement of Photoluminescence Properties. *Angew. Chem., Int. Ed.* **2009**, *48*, 3846–3849.

44 Caravan, P.; Ellison, J. J.; McMurry, T. J.; Lauffer, R. B. Gadolinium(III) Chelates as MRI Contrast Agents: Structure, Dynamics, and Applications. *Chem. Rev.* **1999**, *99*, 2293–2352.

45 Aime, S.; Botta, M.; Fasano, M.; Terreno, E. Prototropic and Water-Exchange Processes in Aqueous Solutions of Gd(III) Chelates. *Acc. Chem. Res.* **1999**, *32*, 941–949.